

Connecting the legs with a spring improves human running economy

Cole S. Simpson¹, Cara G. Welker^{1,2}, Scott D. Uhlrich¹, Sean M. Sketch¹, Rachel W. Jackson², Scott L. Delp^{1,2}, Steve H. Collins¹, Jessica C. Selinger^{2,3,+,*}, and Elliot W. Hawkes^{4,+,*}

¹Stanford University, Department of Mechanical Engineering, Stanford, CA, 94305, USA

²Stanford University, Department of Bioengineering, Stanford, CA, 94305, USA

³Queen's University, School of Kinesiology and Health Studies, Kingston, Ontario, Canada

⁴University of California, Santa Barbara, Department of Mechanical Engineering, Santa Barbara, CA, USA

⁺these authors contributed equally to this work

^{*}Correspondence and requests for materials should be addressed to E.W.H.

(ewhawkes@ucsb.edu) or J.C.S. (j.selinger@queensu.ca)

Key words: biomechanics, energetic cost, metabolic cost, gait, running, assistive device

Summary statement

Connecting the legs with a spring assists runners in swinging their legs, enabling them to take faster, shorter, more efficient strides.

Abstract

Human running is inefficient. For every ten calories burned, less than one is needed to maintain a constant forward velocity—the remaining energy is, in a sense, wasted. The majority of this wasted energy is expended to support the bodyweight and redirect the center of mass during the stance phase of gait. An order of magnitude less energy is expended to brake and accelerate the swinging leg. Accordingly, most devices designed to increase running efficiency have targeted the costlier stance phase of gait. An alternative approach is seen in nature: spring-like tissues in some animals and humans are believed to assist leg swing. While it has been assumed that such a spring simply offloads the muscles that swing the legs, thus saving energy, this mechanism has not been experimentally investigated. Here we show that a spring, or ‘exotendon’, connecting the legs of a human reduces the energy required for running by $6.4 \pm 2.8\%$, and does so through a complex mechanism that produces savings beyond those associated with leg swing. The exotendon applies assistive forces to the swinging legs, increasing the energy optimal stride frequency. Runners then adopt this frequency, taking faster and shorter strides, and reduce the joint mechanical work to redirect their center of mass. Our study shows how a simple spring improves running economy through a complex interaction between the changing dynamics of the body and the adaptive strategies of the runner, highlighting the importance of considering each when designing systems that couple human and machine.

Introduction

Running expends more energy than any other commonly used form of locomotion, including walking, swimming, and flying (Alexander, 2005; Butler, 2016; Schmidt-Nielsen, 1972) (Fig. 1A). In running humans, only a small amount of the metabolic energy expended does net external work on the environment; this energy is used to overcome aerodynamic drag and represents less than 8% of the total energy expended (Fig. 1B) (Davies, 1980; Pugh, 1970). The remaining energy is ‘wasted’ in the sense that it is expended by processes that do no useful external work on the environment. According to studies that attempt to partition the energy

expended by these processes, most of the wasted energy (65-82%) is used to brake and accelerate the center of mass, both vertically and fore-aft, a process that occurs each stance phase (Arellano and Kram, 2014). A smaller portion is used to swing the legs (Arellano and Kram, 2014; Marsh et al., 2004; Modica and Kram, 2005), with the current best estimate at 7% (Arellano and Kram, 2014).

Given the inefficiency of running, many devices have been designed to reduce a runner's metabolic energy expenditure, with most targeting the largest costs—redirecting the center of mass and supporting the weight during the stance phase of gait. These devices can be either active or passive. Active devices inject energy from an external source to reduce the amount of energy expended by the human, even while the total energy expended by the human-plus-device may increase. For example, exoskeleton robots use motors in parallel with human muscles (Lee et al., 2017; Zhang et al., 2017). However, these active exoskeleton robots usually use offboard motors and power sources, which prevent them from being autonomous. Other examples of active devices include mechanisms with accelerated masses (Sugar et al., 2015) and jet packs (Kerestes and Sugar, 2015). No actively powered device, however, has consistently reduced the energy required for a human to run while carrying the full weight of the device. Passive devices, in contrast, seek to reduce the energy required by the human to run by storing and returning energy to create a more efficient human-plus-device system. An early example is a running surface with stiffness tuned to minimize energy lost during impacts (Kerdok et al., 2002; McMahon and Greene, 1979). Another passive assistance strategy involves using springs in parallel with the legs (Dollar and Herr, 2008; Grabowski and Herr, 2009), but this approach has yielded mixed results. Most recently, a shoe with spring-like foam and an assistive carbon fiber plate resulted in a 4% improvement in running economy (Hoogkamer et al., 2017; Hoogkamer et al., 2019), the largest savings for a self-contained system across all devices that target costs primarily occurring during stance.

Notably, few devices have been designed that specifically target the metabolic energy expended for leg swing during running, even though numerous researchers hypothesize that passive elastic tissues in animals may reduce the energy required to oscillate limbs. Many quadrupeds have elastic tissues running along the top of the spine and front of the hip that are thought to assist

spinal extension and hip flexion (Alexander et al., 1985; Bennett, 1989) (Fig. 1C). Analogous passive elastic tissues are also in the skin of some fishes (Pabst, 2007) and the wings of birds and insects (Alexander and Bennet-Clark, 1977; Wells, 1993). While no such mechanisms have been identified in humans, studies have correlated less flexibility in the legs and lower back with improved running economy (Craib et al., 1996; Gleim et al., 1990; Jones, 2002). This decreased flexibility might result from increased stiffness of passive elastic tissue spanning the relevant joints. For all of these examples, it is thought that the passive elastic tissues store and return energy during the oscillation of a limb, reducing the effort required to actively brake and accelerate the limb with muscles (Fig. 1D) (Alexander and Bennet-Clark, 1977; Alexander et al., 1985; Bennett, 1989; Craib et al., 1996; Dickinson and Lighton, 1995; Pabst, 2007; Wells, 1993). Interestingly, recent work both in simulation (Welker et al., 2017) and in experiments with a hip-mounted metal torsional spring device (Nasiri et al., 2018) suggest that the savings resulting from assisting swing in humans are comparable to those seen when assisting stance. This is despite the fact that the energy expenditure associated with stance is an order of magnitude larger (Arellano and Kram, 2014). Moreover, the savings associated with assisting swing may actually exceed the expected expenditure associated with swing (Arellano and Kram, 2014), suggesting that the mechanism of savings when assisting swing is not understood.

Here, we first test if a simple spring, or ‘exotendon,’ connecting the legs of a human can reduce whole-body metabolic energy expenditure during running. Next, to elucidate the underlying mechanism of savings, we test the hypothesis that applying moments to assist moving the legs back and forth during swing may in fact reduce costs associated with performing work on the center of mass incurred during the stance phase of gait (Fig. 2). This hypothesis can be explained as follows. During natural running, we expect certain costs to increase with increasing stride frequency, such as costs associated with swinging the legs back and forth at rates higher than the natural frequency (Doke et al., 2005; Kuo, 2001). Other costs we expect to decrease as stride frequency increases, such as costs associated with performing mechanical work on the center of mass to redirect the body in both the vertical and fore aft directions (Kuo, 2001; Kuo et al., 2005; Snyder and Farley, 2011). Therefore, the optimal stride frequency is dictated by a tradeoff between the marginal costs of each. We thus hypothesize that when a device assists leg swing to reduce energy expenditure at a higher stride frequency, the optimal stride frequency will

increase. Adopting this new higher stride frequency will reduce costs that decrease at higher stride frequencies, such as redirecting the body during stance.

Materials and Methods

Device design. We constructed our exotendons out of natural latex rubber surgical tubing (hollow cylindrical tubing, 0.95 cm outer diameter, 0.64 cm inner diameter). Each exotendon consists of a single length of tubing with a 1 cm loop at each end for attachment purposes. To make each loop, we folded the tubing, stretched the loop by hand, and wrapped the looped tubing tightly with electrical tape. Once released, the forces provided by Poisson expansion of the tubing supplement the adhesive, forming a secure connection. We then attached each loop to a 1.6 by 0.5 cm s-shaped stainless-steel carabiner that was clipped to the shoelaces of each participant. The length of each exotendon from end to end of each attachment loop was set to 25% of the participant's leg length, measured as the distance from the top of the anterior superior iliac spine to the medial malleolus of the ankle. Through pilot testing, we found that this length was long enough to avoid breaking and short enough to avoid tripping during running. As this work was our first proof-of-concept for the device, we did not develop a systematic method for determining the optimal stiffness of the device. Instead, we heuristically chose a single stiffness for the device that was stiff enough in piloting to exert noticeable assistive forces, yet compliant enough that it did not highly constrain gait. An exotendon device is shown in Fig. 3 and Supplementary Movie 1.

Designing devices that reliably and accurately apply forces to the human body is a challenge. It often requires overcoming a myriad of difficulties including: aligning device and joint axes (Schiele and van der Helm, 2009), limiting added mass and materials to the body, and comfortably transferring force from rigid devices to often soft and deforming body segments (Sengeh and Herr, 2013). While we could have designed our device to attach more proximally, at the knee or hip for example, we found in piloting that the aforementioned challenges could be largely avoided by affixing our device to the shoes. In addition, attaching more distally on the leg offered two further advantages. First, due to a longer moment arm about the hip, the forces necessary to provide assistive moments to the limb were smaller than if the attachment points were more proximal. Second, more distal placements ensure the line-of-action of the spring is

predominantly along the flexion-extension axis of the hip, minimizing adduction moments on the leg. We note Nasiri et al. (2018) have created an effective hip-mounted device, although the current, largely metal, design must contend with the challenges of added mass and comfortably transferring force from the device to the user.

Device characterization. To determine the force-length relationship of our device, we applied six known forces to one end of a 23 cm exotendon five times each using a pull-linear scale while the other end was fixed. At the same time, the length was recorded with a motion capture system at 270 Hz (Impulse X2E, PhaseSpace, San Leandro, CA, USA). We insured that the displacements achieved exceeded 30 cm (that expected during exotendon running at our experimental speeds). We then fit a linear model to the force-displacement data using least squares regression and computed the coefficient of determination. We found that the forces applied by the exotendon vary nearly linearly with displacement. A linear model fit to the recorded force-displacement data (Fig. 4) was able to account for most of the variance ($R^2 = 0.96$).

To determine how much of the energy stored in a stretched exotendon is returned, we suspended a 2.3 kg mass from one end of a 30 cm exotendon with its other end fixed to a table. We stretched the exotendon to 70 cm (for 40 cm of displacement beyond its free length) and after releasing, measured displacement. We computed the stored potential energy in the stretched exotendon and the gravitational potential energy at the apex of the motion. Comparing these two values gave an energy return of 97%.

Participants. A total of 19 healthy young adults, with no known musculoskeletal or cardiopulmonary impairments, participated in the study (8 females; age: 24.9 ± 2.7 years; height: 174.4 ± 6.9 cm; mass: 67.3 ± 11.0 kg). The study was approved by the Stanford University ethics board and all participants provided written informed consent prior to testing.

Experimental protocols. We conducted four separate experiments to: determine if the exotendon improves running economy (Experiment 1), test for the possibility of a placebo effect

(Experiment 2), investigate the mechanism of energy savings (Experiment 3), and test the safety of the device during over-ground running (Experiment 4).

Experiment 1 – Running economy. To determine if the exotendon improves running economy, we conducted an experiment to compare metabolic energy expenditure with and without the exotendon. Twelve participants (5 females; age: 24.7 ± 2.9 years; height: 177.0 ± 6.7 cm; mass: 69.3 ± 11.4 kg) completed a two-day running protocol. On the first day of testing, we measured participants' leg lengths and constructed personalized exotendons (25% of leg length). Participants were told that the exotendon was designed to improve running efficiency and were told to 'relax into running with the device' and try to 'think about something else' while running. The exotendon was then attached to the participant's shoes (see Device design for attachment location rationale). To habituate participants to the device, they completed a minimum of four 15 m over-ground walking and running trials until they verbally confirmed they were comfortable walking and running with the exotendon. Participants were then instrumented with indirect calorimetry equipment (Quark CPET, Cosmed, Rome, Italy) and completed a 5-minute quiet standing trial, during which baseline metabolic energy expenditure was measured. Participants then completed four 10-minute runs, with 5-minute rests between each, on a treadmill (Woodway, Waukesha, WI) at 2.67 m/s (10 minutes/mile). Though slow for competitive runners, this pace allowed a larger pool of potential participants than a faster pace and is similar to that used in other studies of assistive devices for running (Lee et al., 2017; Nasiri et al., 2018). This pace is also similar to the pace chosen by healthy recreational runners in previous treadmill studies (Kong et al., 2012; Minetti et al., 2015) and to the 2.74 m/s (2.9 m/s for men and 2.5 m/s for women) average running pace measured across 36 million users who ran 1.5 billion kilometers (Strava, San Francisco, CA, USA; <https://blog.strava.com/press/2018-year-in-sport/>, accessed July 11, 2019). The runs alternated between 'natural running' (without an exotendon) and 'exotendon running' (with an exotendon), with the first running condition randomly assigned. The second day of testing was identical to the first for each participant. We define a trial as the comparison between consecutive natural and exotendon runs resulting in four trials over the two-day experiment. During runs, we recorded sagittal plane video, which we later used to determine runners' stride frequencies. However, in 5 of 12 participants, due to equipment

availability, we recorded stride frequency using an accelerometer (Trigno IM, Delsys Inc., Natick, MA, USA) mounted on the dorsal surface of the foot.

Experiment 2 – Placebo effect. To determine if a placebo effect could explain the changes in running economy observed in Experiment 1, we conducted a separate experiment to compare metabolic energy expenditure during running with and without a placebo exotendon. Four naïve participants (2 females; age: 24 ± 2.2 years; height: 168.3 ± 2.5 cm; mass: 60.1 ± 10.8 kg) completed a two-day running protocol that was identical to Experiment 1. The only difference was that participants ran with an exotendon that had a stiffness two orders of magnitude lower than the original exotendon (5 N/m versus 120 N/m, respectively), and therefore provided negligible assistive moments to the limbs. The length of each placebo exotendon was still set to 25% of participant leg length.

Experiment 3 – Mechanism. To investigate how the exotendon reduces energy expenditure, we conducted an experiment to test how running mechanics, energetics, and muscle activity change during exotendon running. Four participants (2 females; age: 25.0 ± 1.6 years; height: 179.5 ± 7.4 cm; mass: 75.3 ± 13.7 kg), randomly selected from the 12 that participated in Experiment 1, completed an additional third day of testing. During this testing day, kinematic, kinetic, electromyographical (EMG), and metabolic data were recorded during running with and without the exotendon at a range of stride frequencies.

All runs were completed at 2.67 m/s on an instrumented treadmill (Bertec Corporation, Columbus, OH, USA) to allow for collection of ground reaction forces (2000 Hz). Kinematic data were recorded at 100 Hz using a 9-camera optical motion tracking system (Motion Analysis Corporation, Santa Rosa, CA, USA). Anatomical reflective markers were placed bilaterally on the 2nd and 5th metatarsal heads, calcanei, malleoli, femoral epicondyles, anterior and posterior superior iliac spines, and acromion processes, as well as on the C7 vertebrae. An additional 16 tracking markers, arranged in clusters, were placed on the shanks and thighs of both legs. Markers on the medial malleoli and femoral epicondyles were removed following the static trial. EMG data were recorded (Trigno IM, Delsys Inc., Natick, MA, USA) at 2000 Hz from the following 15 muscles of a single limb: peroneus, soleus, medial and lateral gastrocnemii, tibialis

anterior, medial and lateral hamstrings, gluteus medius and maximus, vastus lateralis and medialis, rectus femoris, sartorius, adductor group, and iliopsoas. EMG electrodes were placed in accordance to SENIAM guidelines (Hermens et al., 1999). Metabolic power was measured using indirect calorimetry (Quark CPET, Cosmed, Rome, Italy).

To warm up, participants ran without an exotendon for 5 minutes on the treadmill. Next, participants completed a series of maximum voluntary contractions (MVCs) for later normalization of EMG signals. These MVCs included five maximum height jumps and five sprints (Suydam et al., 2017), in addition to one isometric and three isokinetic maximum contractions of the hamstrings, adductor group, tibialis anterior, peroneus, hip flexors (with both a flexed knee and extended knee), and hip abductors. We then recorded motion capture marker positions and ground reaction forces during a static standing trial for later scaling of a musculoskeletal model. As in Experiment 1, participants were habituated to the device through a series of over-ground walking and running trials. Participants were then instrumented with indirect calorimetry equipment and a 5-minute quiet standing trial was recorded to capture baseline metabolic energy expenditure.

Participants then completed two 7-minute runs, one ‘natural running’ (without an exotendon) and one ‘exotendon running’ (with an exotendon), with a 5-minute rest between and the order randomly assigned. Kinematic, kinetic, EMG, and metabolic data were recorded. Self-selected stride frequency was computed during the last minute of each run from the instrumented treadmill force signals with a custom MATLAB script (Mathworks Inc., Natick, MA, USA). We will refer to these self-selected stride frequencies as *natural self-selected stride frequency* and *exotendon self-selected stride frequency*.

To investigate how the relationship between stride frequency and metabolic power changed when running with an exotendon, participants next completed six additional 7-minute runs during which step frequency was prescribed using an auditory metronome, along with visual cues provided by a monitor in front of the treadmill. Participants ran at three prescribed stride frequencies during both natural and exotendon running. For the natural running conditions, the following three stride frequencies were prescribed: i. the participant’s natural self-selected stride

frequency; ii. the participant's exotendon self-selected stride frequency, which was higher than the natural self-selected stride frequency; and iii. a stride frequency lower than the natural self-selected stride frequency. The change from the natural self-selected stride frequency to the lower stride frequency was set to the percent difference between the natural self-selected stride frequency and the exotendon self-selected stride frequency. For the exotendon running conditions, the following three stride frequencies were prescribed: i. the participant's exotendon self-selected stride frequency; ii. the participant's natural self-selected stride frequency; and iii. a stride frequency higher than the exotendon self-selected stride frequency. The change from exotendon self-selected stride frequency to the higher stride frequency was similarly set to the percent difference between the natural self-selected stride frequency and exotendon self-selected stride frequency.

Experiment 4 – Over-ground test. To test whether the exotendon can safely be used in the real-world, we conducted an experiment to monitor fall risk during outdoor running. Four participants (2 females; age: 27.8 ± 1.3 years; height: 172.6 ± 6.1 cm; mass: 66.7 ± 8.0 kg), who had previous experience with the exotendon through pilot testing or participation in Experiment 1, ran with a modified exotendon for 6 km on suburban streets. The modified exotendon, which attached directly to the ankle via a compression brace, was reported to be more comfortable than the original exotendon, which attached directly to the shoelaces. Moving the attachment point off the shoes also reduced wear of the shoelaces caused by sliding of the carabiner. This small change in attachment point was not expected to have a significant effect on running economy. The number of tripping and falling incidents were recorded.

A Note on Device Optimization. In supplementary pilot experiments (not presented here), we did attempt to perform human-in-the-loop optimization to determine the optimal exotendon length and stiffness. Four participants (two who had previously completed Experiment 1 and two naïve participants) completed a protocol similar to that described in Zhang et al. (Zhang et al., 2017). We were unable to identify length and stiffness combinations with better performance than our standard device in the four pilot participants. One possible explanation is that our chosen device parameters were indeed near optimal. A more likely explanation is that our optimization protocol did not allow sufficient time for the algorithm to converge on the most efficient set of exotendon

parameters. Also, learning effects may have interfered with the optimization due to the relatively short exposure to each exotendon. Another possible explanation is that participants were more risk averse in running with our device and thus adopted control strategies that prioritized stability (not falling) over efficiency. Parsing the different effects of human-in-the-loop optimization is left for future work.

Data analysis.

Experiment 1 – Running economy.

Metabolics. We computed the gross metabolic power (energy expenditure) from indirect calorimetry (Brockway, 1987) by averaging data from the last two minutes of each experimental run. Baseline metabolic power, calculated as the average metabolic power during the last two minutes of the rested standing trial, was subtracted from our gross metabolic power measures to get net metabolic power during each run. We then computed the percent change in net metabolic power, from natural running to exotendon running for each of the four trials. We used two-tailed, one-sample t-tests, with a Holm-Šidák correction, to determine if percent changes in net metabolic power were significant.

Stride frequency. We manually determined average stride frequency from video recordings by counting the strides taken and dividing by the time elapsed. When foot mounted accelerometers were instead used to compute stride frequency, we bandpass filtered accelerometer data (4th order, zero-phase shift Butterworth, 2-20 Hz), summed the X, Y and Z accelerations, identified peak accelerations, and computed stride frequency as one over the average time between peaks. Average stride frequency measures were not statistically different between the two measurement methods.

Experiment 2 – Placebo effect.

Metabolics. We performed the same metabolic analyses as described in Experiment 1.

Experiment 3 – Mechanism.

Metabolics. We performed the same metabolic analyses as described in Experiment 1 to determine the average net metabolic power for each run. To determine the effect of altering

stride frequency, we computed the percent change in average net metabolic power for each enforced stride frequency, both with and without an exotendon, relative to natural running (without an exotendon and with no enforced stride frequency). For each participant, we then used least squares regression to find the best-fit quadratic curves relating net metabolic power to stride frequency for both exotendon and natural running. We calculated the stride frequencies at the minima of the natural running and exotendon running best-fit curves, which we will refer to as the *natural optimal stride frequency* and the *exotendon optimal stride frequency*, respectively. To determine if the exotendon shifted the optimal stride frequency, we performed two-tailed paired t-tests comparing exotendon optimal stride frequency to natural optimal stride frequency. Using all participant data, we also solved for best-fit quadratic curves relating net metabolic power to stride frequency for both exotendon and natural running, and calculated the 95% bootstrap confidence intervals for these across participant curves. Note that each quadratic curve is fit to only three data points. While this is an overfit to our data, we have chosen to do so because previous studies have shown that running metabolic cost varies quadratically with stride frequency (Högberg, 1952; Hunter and Smith, 2007; Snyder and Farley, 2011). The curve fits are only used to interpolate the stride frequency associated with the minimum metabolic cost.

Musculoskeletal modeling. Joint-level kinematics, kinetics, and mechanical powers were computed using a modified musculoskeletal model (Rajagopal et al., 2016) in OpenSim 3.3 (Delp et al., 2007). Of the original 37 model degrees of freedom, we locked 18 including ankle eversion, toe flexion, and all those associated with the arms, leaving us with a 19 degree-of-freedom model. We generated subject-specific models by scaling the generic model to match the anthropometry of each subject during a standing static trial. For scaling, ankle and knee joint centers were calculated as the midpoint of the calcanei markers and femoral epicondyle markers, respectively, while the hip joint centers were calculated using a regression model based on the marker positions of the posterior and anterior superior iliac spines (Harrington et al., 2007). After low-pass filtering the marker positions at 15 Hz (4th order, zero-phase shift Butterworth), we computed joint angles using the OpenSim inverse kinematics tool. This tool uses a weighted least squares algorithm to pose the model in a way that minimizes the error between model and experimental marker locations. Joint moments were computed using the OpenSim inverse dynamics tool, which uses ground reaction forces and moments, joint angles from inverse

kinematics, and classical equations of motion to solve for intersegmental moments. The joint angles used as input were low-pass filtered at 15 Hz (6th order, zero-phase shift Butterworth), and ground reaction forces and moments were low-pass filtered at 15 Hz (4th order, zero-phase shift Butterworth).

We modeled the exotendon in OpenSim as a linear path spring with a deadband range equal to its slack length. Though no real material behaves as a perfect linear spring, we determined in benchtop tests that the stiffness of our device is roughly linear ($R^2 = 0.96$) and returns 97% of the energy stored in it. The spring forces were applied to the calcaneus body of each foot at the location of the band attachment marker from the static trial. The length and stiffness of the modeled exotendon was scaled for each participant. Inverse dynamics were first computed without the modeled exotendon to determine the total joint moments required to produce the resultant motion and ground reaction forces, referred to as *exotendon running total moments*. Inverse dynamics were then recomputed with the modeled exotendon for all exotendon runs to determine the moments produced solely by biological muscle and tissue, referred to as the *biological moments*. The moments applied by the exotendon were computed as the difference between the exotendon running total moments and biological moments, referred to as *exotendon moments*. We confirmed that the exotendon did approximately zero net work during a gait cycle (-0.04 J) in a representative participant. This value can be non-zero because the gait cycle may not end exactly where it began. Powers were then computed at each joint by multiplying moments by angular velocities.

Participants' average joint angles and moments as a function of gait cycle for the hip, knee and ankle were calculated from the last minute of each run. To do this, we averaged across strides after normalizing each stride time to 100% gait cycle, computed as the time from heel strike to subsequent heel strike on a single leg. Strides were excluded from these average trajectories if the value of the measure exceeded 5 standard deviations from the mean at any time point in the stride. This resulted in the removal of 3% of strides on average for all runs and participants. Joint powers were then computed from the averaged joint angles and moments for each participant. Joint powers and moments were then normalized to body mass and across-participant average trajectories were computed.

We next computed the average absolute natural running and exotendon running moments and powers (both biological and exotendon) during the stance and swing phases of gait. We note that because these values are time averaged, the relative length of the stride does not affect their magnitude. We tested for differences between natural running and exotendon running (again, both biological and exotendon) using two-tailed paired t-tests with Holm-Šidák corrections.

We performed these analyses, comparing joint moment and powers during the swing and stance phases of gait both with and without the exotendon, as a means of estimating effort during each phase. Metabolic power, measured using indirect calorimetry, is our most direct measure of energy expenditure, but cannot be used to distinguish stance and swing expenditures; their effects are intermingled during the long sampling period of indirect calorimetry. Instead we analyzed the mechanical requirements of the body (joint moments) during each phase of gait. Previous studies have shown strong correlations between metabolic power and joint moment (Doke and Kuo, 2007), but we note that reduced joint moments do not guarantee reduced metabolic rate (Robertson et al., 2014).

Electromyography. Electromyograms from each muscle were bandpass filtered at 30-500 Hz (4th order, zero-phase shift Butterworth), rectified, and then low-pass filtered at 6 Hz (4th order, zero-phase shift Butterworth) to create linear envelopes. Envelopes were then normalized to the peak signal from the MVCs (Suydam et al., 2017) to compute muscle activities. We then averaged muscle activities across strides from the final minute of each run, then normalized to 100% of the gait cycle. Strides in which the muscle activities exceeded 5 standard deviations from the mean for any time point were excluded from the average curve. All remaining EMG signals were visually examined and excluded if they appeared corrupted. Overall, 8% were excluded, with no bias towards exotendon or natural running. All processing was performed using custom MATLAB scripts. We also computed average muscle activities during the stance and swing phase of gait, both for natural and exotendon running. We used two-tailed paired t-tests with Holm-Šidák corrections to compare activity during natural and exotendon running, during both stance and swing.

Results

Experiment 1 – Running economy. We found that connecting the legs of a running human with a simple spring improved running economy by $6.4 \pm 2.8\%$ ($n=12$, $p=6.9 \times 10^{-6}$, one-sample t-test, Fig. 5A). During the first trial of the first day, participants showed no metabolic savings when running with an exotendon compared to natural running. However, by the end of the second trial, participants were expending $3.8 \pm 5.4\%$ less energy during exotendon running compared to natural running ($n = 12$, $p = 0.034$, one-sample t-test). Metabolic savings continued to increase on the second testing day, with all participants achieving savings by the end of the second trial of the second testing day. By the end of our protocol, stride frequency increased by an average of $7.7 \pm 3.5\%$ when wearing an exotendon ($n=12$, $p = 1.1 \times 10^{-5}$, paired t-test, Fig. 5B).

Experiment 2 – Placebo effect. The placebo exotendon did not improve running economy ($n=4$, $p=0.88$, one-sample t-test, Fig. S1).

Experiment 3 – Mechanism. The exotendon significantly increased the optimal stride frequency ($+8.1\%$, $p=3.7 \times 10^{-3}$, $n=4$, paired t-test, Fig. 6A), and all participants adapted toward the new optimum. The exotendon reduced biological hip and knee moments during swing ($p=2.3 \times 10^{-3}$, 2.5×10^{-3} , respectively, paired t-test) and stance ($p=4.1 \times 10^{-3}$, 8.1×10^{-5} , respectively, paired t-test) (Fig. 6B, Fig. 7 and Fig. S2). Interestingly, average knee moments during stance decreased ($p=4.4 \times 10^{-4}$, paired t-test), even when the exotendon was applying negligible moments, likely because runners adopted a higher stride frequency, as our hypothesis suggests. In addition, biological joint powers at the knee decreased during swing and stance ($p=7.7 \times 10^{-3}$, 1.7×10^{-3} , respectively, paired t-test, Fig. 7), as did ankle joint power during stance ($p=8.4 \times 10^{-3}$, paired t-test, Fig. 7). Corresponding reductions in muscle activities were not significant, possibly due to the low signal-to-noise ratio (Figs. S3 and S4).

Experiment 4 – Over-ground test. To test the safety and potential real-world applicability of our exotendon, four participants each ran 6 km on city streets with a modified exotendon (see Materials and Methods, Experiment 4); no tripping incidents occurred.

Discussion

We found that a simple spring connecting the legs of a running human can improve overall economy. Moreover, the exotendon appears to not simply reduce the cost of swinging the limbs. Instead, we found that savings are the product of a complex interaction between the mechanics of the simple device and the adaptive strategies of the runner. We show that the exotendon increases the energy optimal stride frequency, which runners then adopt. At this new stride frequency, the mechanical work of redirecting the center of mass during stance is reduced—shorter strides result in a reduction of biological joint moments and powers. This suggests that the metabolic cost associated with this mechanical work is reduced, and the overall improvement of economy is not derived solely from reducing the cost of swinging the legs. Our findings help explain why devices designed to assist the low expenditure costs of leg swing (Nasiri et al., 2018), yield greater improvements in overall running economy than those that directly assist the larger costs of redirecting the center of mass and supporting the bodyweight (Hoogkamer et al., 2017).

Stated more generally, during natural running, low-expenditure components can have high expenditures when a gait parameter (such as stride frequency) is changed outside of the preferred range. These sharp increases in expenditure (the marginal costs) act as a constraint, preventing adjustment to the gait parameter. During assisted running, this constraint is relaxed, freeing the runner to reduce expenditures associated with the high-expenditure components of gait (such as center of mass redirection) and achieve more efficient gait patterns overall. Critically, the associated savings can be large—much larger than would be expected from savings directly associated with a low-expenditure component of gait (Fig. 2).

A primary limitation of our study is the difficulty of disentangling, and quantifying, costs associated with one component of gait from another during human running. In particular we refer to two costs. One is the cost associated with performing work to redirect the center of mass both vertically and fore-aft, which we expect to primarily occur during the stance phase of gait and expect to decrease with increasing stride frequency (or decreasing step length). The other is the cost to move the legs back and forth during the swing phase of gait, which we expect to increase

with increasing stride frequency. While there is a body of modeling and experimental evidence to broadly support the importance and tradeoff of these two competing costs (Doke and Kuo, 2007; Kuo, 2001; Kuo et al., 2005; Snyder and Farley, 2011), in reality they cannot be measured in isolation. For example, at higher step frequencies we also expect greater ‘force rate costs.’ This cost is associated with more rapidly turning muscles on and off, with the more rapid activation cycling hypothesized to require more costly calcium pumping (Doke and Kuo, 2007; Doke et al., 2005; Pontzer, 2007). This cost would be incurred by muscles involved in center of mass redirection and body weight support, as well as muscles responsible for swing. Although joint moments and powers were reduced during both stance and swing, this does not directly map to reductions in cost because of complications like force-rate costs, as well as other considerations such as biological tendon energy storage and return, or isometric force production. While we expect force rate costs to increase while wearing the exotendon due to the shortened ground contact time, the increased cost is mostly mitigated by changes in the effective moment arms of the joints. Notably, considering these costs does not negate our proposed mechanism of savings; even in their presence, our results are consistent and compatible with our hypothesized mechanism of savings (Fig S5).

Adding to the challenge of disentangling costs was the limitation that we did not find significant changes in muscle activity, despite reductions in metabolic and mechanical powers during exotendon running. A similar study was also unable to verify changes in muscle activity while testing an exosuit that improved running economy by 5% in 8 participants (Lee et al., 2017). This apparent discrepancy in our study is likely due to the distribution of the exotendon’s effect on metabolic power consumption across a large number of muscles. This diluted effect might be difficult to verify in EMG signals with relatively high variability. Additionally, recorded muscle activity may not have changed despite decreased joint moments if changes occurred in non-superficial muscles that are unmeasurable with surface EMG (Bernstein, 1967; Martelli et al., 2015; Simpson et al., 2015). Alternatively, because metabolic power results from a combination of factors including muscle activation, muscle fiber length and velocity (kinematics), and mechanical work done by the muscle fibers (Umberger, 2010; Umberger et al., 2003), muscle activity need not change though joint moments and metabolic power did.

An open question is whether our device would be more or less effective at higher running speeds. Our current study was conducted at one, relatively slow, speed. At higher running speeds the amplitude and frequency of leg swing increase (Schache et al., 2014) leading to greater leg swing costs (Doke and Kuo, 2007) that the device may help offset. However, the marginal costs associated with the work to redirect the center of mass and force rate costs would likely change with running speed, making the net effect unclear. To further complicate the situation, other kinematic changes occur at high speeds. For example, during natural running at faster speeds greater knee flexion is evident at the rearward extent of leg swing, reducing the leg's moment of inertia about the hip and potentially reducing swing costs. The exotendon may in fact hinder this more exaggerated knee flexion at higher speeds, leaving the net effect on leg swing costs uncertain. Although the effect of our device at faster running speeds is somewhat unclear, the improvement in economy at the tested speed does imply that recreational runners may be able to run faster and further with our device. A runner, with a natural pace of 2.7 m/s and a marathon finishing time of 4:20, could expect a 6% improvement in economy with our device, theoretically leading to a decrease in their finishing time to around the 4-hour mark (Hoogkamer et al., 2016; Kipp et al., 2019).

Our study shows how a spring designed to assist leg swing can significantly improve human running economy through a complex mechanism of savings. The device changes the relationship between stride frequency and energy expenditure, driving the runner to discover new locomotor strategies. This change in turn reduces the mechanical work the runner does to both swing the legs and redirect the center of mass, resulting in overall greater efficiency than anticipated. Our exotendon could serve as an affordable and low-tech assistive device to improve human running performance, or a simple and robust intervention to further explore the complexities of human gait and human-machine interactions. More broadly, our study shows that a simple device can create unexpected and complex interactions between the dynamics of the body and the adaptive strategies of the individual—an important reminder for all who seek to augment humans.

Acknowledgments: Thanks to Rachel Troutman for assistance running pilot studies, Michael Raitor for comments, insights, and enthusiasm, and Allison Okamura for always supporting her students, even if they stray far from her area of expertise.

Funding: Funding for this work was provided by National Science Foundation Graduate Research Fellowships [DGE-114747 to C.S.S. and S.D.U., DGE-1656518 to C.G.W.], a Stanford Bioengineering Fellowship [C.G.W.], a Stanford Graduate Fellowship [S.D.U.], a Pfeiffer Research Foundation Stanford Interdisciplinary Graduate Fellowship affiliated with the Wu Tsai Neurosciences Institute [S.M.S.], National Institutes of Health Big Data to Knowledge Center [U54 EB020405 to S.L.D.], the National Center for Simulation in Rehabilitation Research [P2C HD065690 to S.L.D.], and National Science Foundation [CMMI-1818602 to S.H.C.].

Author contributions: CSS and EWH conceived of the device. CSS, CGW, JCS, and EWH conceptualized the study. All authors contributed to experimental design. CSS, CGW, and SDU conducted the experiments. CSS, CGW, SDU, and SMS analyzed the results, with supervision from RWJ, SHC, JCS, and EWH. CSS, CGW, SDU, JCS, and EWH drafted the manuscript. All authors reviewed and edited the manuscript.

Competing interests: No competing interests declared.

Data and materials availability: The data that support the findings of this study are available from the authors on request.

References

- Alexander, R. M.** (2005). Models and the scaling of energy costs for locomotion. *J. Exp. Biol.* **208**, 1645–1652.
- Alexander, R. M. and Bennet-Clark, H. C.** (1977). Storage of elastic strain energy in muscle and other tissues. *Nature* **265**, 114–117.
- Alexander, R. M., Dimery, N. J. and Ker, R. F.** (1985). Elastic structures in the back and their role in galloping in some mammals. *J. Zool. London* **207**, 467–482.
- Arellano, C. J. and Kram, R.** (2014). Partitioning the metabolic cost of human running: A task-by-task approach. In *Integrative and Comparative Biology*, pp. 1084–1098. Oxford University Press.
- Bennett, M. B.** (1989). A possible energy- saving role for the major fascia of the thigh in

- running quadrupedal mammals. *J. Zool.* **219**, 221–230.
- Bernstein, N. A.** (1967). *The Co-ordination and regulation of movements*. Pergamon Press Ltd.
- Brockway, J. M.** (1987). Derivation of formulae used to calculate energy expenditure in man. *Hum. Nutr. Clin. Nutr.* **41**, 463–71.
- Butler, P. J.** (2016). The physiological basis of bird flight. *Philos. Trans. R. Soc. B Biol. Sci.* **371**,.
- Craib, M. W., Mitchell, V. A., Fields, K. B., Cooper, T. R., Hopewell, R. and Morgan, D. W.** (1996). The association between flexibility and running economy in sub-elite male distance runners. *Med. Sci. Sports Exerc.* **28**, 737–743.
- Davies, C. T.** (1980). Effects of wind assistance and resistance on the forward motion of a runner. *J. Appl. Physiol.* **48**, 702–709.
- Delp, S. L., Anderson, F. C., Arnold, A. S., Loan, P., Habib, A., John, C. T., Guendelman, E. and Thelen, D. G.** (2007). OpenSim: open-source software to create and analyze dynamic simulations of movement. *IEEE Trans. Biomed. Eng.* **54**, 1940–50.
- Dickinson, M. H. and Lighton, J. R. B.** (1995). Muscle Efficiency and Elastic Storage in the Flight Motor of *Drosophila*. *Science (80-.)*. **268**, 87–90.
- Doke, J. and Kuo, A. D.** (2007). Energetic cost of producing cyclic muscle force, rather than work, to swing the human leg. *J. Exp. Biol.* **210**, 2390–2398.
- Doke, J., Donelan, J. M. and Kuo, A. D.** (2005). Mechanics and energetics of swinging the human leg. *J. Exp. Biol.* **208**, 439–445.
- Dollar, A. M. and Herr, H.** (2008). Design of a quasi-passive knee exoskeleton to assist running. In *2008 IEEE/RSJ International Conference on Intelligent Robots and Systems, IROS*, pp. 747–754.
- Full, R.** (1989). Mechanics and energetics of terrestrial locomotion: bipeds to polypeds. In *Energy Transformation in Cells and Animals*, pp. 175–182.
- Gleim, G. W., Stachenfeld, N. S. and Nicholas, J. A.** (1990). The influence of flexibility on the economy of walking and jogging. *J. Orthop. Res.* **8**, 814–823.
- Grabowski, A. M. and Herr, H. M.** (2009). Leg exoskeleton reduces the metabolic cost of human hopping. *J. Appl. Physiol.* **107**, 670–678.
- Harrington, M. E., Zavatsky, A. B., Lawson, S. E. M., Yuan, Z. and Theologis, T. N.** (2007). Prediction of the hip joint centre in adults, children, and patients with cerebral palsy based

on magnetic resonance imaging. *J. Biomech.* **40**, 595–602.

- Hermens, H. J., Freriks, B., Merletti, R., Stegeman, D., Blok, J., Rau, G., Disselhorst-Klug, C. and Hägg, G.** (1999). European recommendations for surface electromyography. *Roessingh Res. Dev.* **8**, 13–54.
- Högberg, P.** (1952). How do stride length and stride frequency influence the energy-output during running? *Arbeitsphysiologie* **14**, 437–441.
- Hoogkamer, W., Kipp, S., Spiering, B. A. and Kram, R.** (2016). Altered running economy directly translates to altered distance-running performance. *Med. Sci. Sports Exerc.* **48**, 2175–2180.
- Hoogkamer, W., Kipp, S., Frank, J. H., Farina, E., Luo, G. and Kram, R.** (2017). New Running Shoe Reduces the Energetic Cost of Running. *Med. Sci. Sport. Exerc.* **49**, 195.
- Hoogkamer, W., Kipp, S. and Kram, R.** (2019). The Biomechanics of Competitive Male Runners in Three Marathon Racing Shoes: A Randomized Crossover Study. *Sport. Med.* **49**, 133–143.
- Hunter, I. and Smith, G. A.** (2007). Preferred and optimal stride frequency, stiffness and economy: Changes with fatigue during a 1-h high-intensity run. *Eur. J. Appl. Physiol.* **100**, 653–661.
- Jones, A. M.** (2002). Running economy is negatively related to sit-and-reach test performance in international-standard distance runners. / L' économie de course est en relation négative avec la performance au test de souplesse "sit and reach" chez des coureurs de fond de niv. *Int. J. Sports Med.* **23**, 40–43.
- Kerdok, A. E., Biewener, A. A., McMahon, T. A., Weyand, P. G. and Herr, H. M.** (2002). Energetics and mechanics of human running on surfaces of different stiffnesses. *J. Appl. Physiol.* **92**, 469–478.
- Kerestes, J. and Sugar, T. G.** (2015). Enhanced Running Using a Jet Pack. In *International Design Engineering Technical Conferences and Computers and Information in Engineering Conference*, p. V05AT08A006. ASME.
- Kipp, S., Kram, R. and Hoogkamer, W.** (2019). Extrapolating Metabolic Savings in Running: Implications for Performance Predictions. *Front. Physiol.* **10**, 1–8.
- Kong, P. W., Koh, T. M. C., Tan, W. C. R. and Wang, Y. S.** (2012). Unmatched perception of speed when running overground and on a treadmill. *Gait Posture* **36**, 46–48.

- Kuo, A. D.** (2001). A Simple Model of Bipedal Walking Predicts the Preferred Speed–Step Length Relationship. *J. Biomech. Eng.* **123**, 264–269.
- Kuo, A. D., Donelan, J. M. and Ruina, A.** (2005). Energetic consequences of walking like an inverted pendulum: step-to-step transitions. *Exerc. Sport Sci. Rev.* **33**, 88–97.
- Lee, G., Kim, J., Panizzolo, F. A., Zhou, Y. M., Baker, L. M., Galiana, I., Malcolm, P. and Walsh, C. J.** (2017). Reducing the metabolic cost of running with a tethered soft exosuit. *Sci. Robot.* **2**, eaan6708.
- Marsh, R. L., Ellerby, D. J., Carr, J. A., Henry, H. T. and Buchanan, C. I.** (2004). Partitioning the Energetics of Walking and Running: Swinging the Limbs Is Expensive. *Science (80-.).* **303**, 80–83.
- Martelli, S., Calvetti, D., Somersalo, E., Viceconti, M. and Sheffield, S.** (2015). Stochastic modelling of muscle recruitment during activity. *Interface Focus.*
- McMahon, T. A. and Greene, P. R.** (1979). The influence of track compliance on running. *J. Biomech.* **12**, 893–904.
- Minetti, A. E., Gaudino, P., Seminati, E. and Cazzola, D.** (2013). The cost of transport of human running is not affected, as in walking, by wide acceleration/deceleration cycles. *J. Appl. Physiol.* **114**, 498–503.
- Minetti, A. E., Boldrini, L., Brusamolin, L., Zamparo, P. and McKee, T.** (2015). A feedback-controlled treadmill (treadmill-on-demand) and the spontaneous speed of walking and running in humans. *J. Appl. Physiol.* **95**, 838–843.
- Modica, J. R. and Kram, R.** (2005). Metabolic energy and muscular activity required for leg swing in running. *J. Appl. Physiol.* **98**, 2126–2131.
- Nasiri, R., Ahmadi, A. and Ahmadabadi, M. N.** (2018). Reducing the energy cost of human running using an unpowered exoskeleton. *IEEE Trans. Neural Syst. Rehabil. Eng.* **26**, 2026–2032.
- Pabst, D. A.** (2007). Springs in Swimming Animals. *Am. Zool.* **36**, 723–735.
- Pontzer, H.** (2007). Predicting the energy cost of terrestrial locomotion: a test of the LiMb model in humans and quadrupeds. *J. Exp. Biol.* **210**, 484–494.

- Pugh, L. G. C. E.** (1970). Oxygen intake in track and treadmill running with observations on the effect of air resistance. *J. Physiol.* **207**, 823–835.
- Rajagopal, A., Dembia, C. L., DeMers, M. S., Delp, D. D., Hicks, J. L. and Delp, S. L.** (2016). Full-Body Musculoskeletal Model for Muscle-Driven Simulation of Human Gait. *IEEE Trans. Biomed. Eng.* **63**, 2068–2079.
- Robertson, B. D., Farris, D. J. and Sawicki, G. S.** (2014). More is not always better: Modeling the effects of elastic exoskeleton compliance on underlying ankle muscle-tendon dynamics. *Bioinspiration and Biomimetics* **9**, 46018.
- Schache, A. G., Dorn, T. W., Williams, G. P., Brown, N. A. T. and Pandy, M. G.** (2014). Lower-Limb Muscular Strategies for Increasing Running Speed. *J. Orthop. Sport. Phys. Ther.* **44**, 813–824.
- Schiele, A. and van der Helm, F. C. T.** (2009). Influence of attachment pressure and kinematic configuration on pHRI with wearable robots. *Appl. Bionics Biomech.* **6**, 157–173.
- Schmidt-Nielsen, K.** (1972). Locomotion: Energy Cost of Swimming, Flying, and Running. *Science (80-.)*. **177**, 222–228.
- Sengeh, D. M. and Herr, H.** (2013). A variable-impedance prosthetic socket for a transtibial amputee designed from magnetic resonance imaging data. *J. Prosthetics Orthot.* **25**, 129–137.
- Simpson, C. S., Hongchul Sohn, M., Allen, J. L. and Ting, L. H.** (2015). Feasible Muscle Activation Ranges Based on Inverse Dynamics Analyses of Human Walking. *J. Biomech.* BMD1401187.
- Snyder, K. L. and Farley, C. T.** (2011). Energetically optimal stride frequency in running: the effects of incline and decline. *J. Exp. Biol.* **214**, 2089–2095.
- Sugar, T. G., Bates, A., Holgate, M., Kerestes, J., Mignolet, M., New, P., Ramachandran, R. K., Redkar, S. and Wheeler, C.** (2015). Limit Cycles to Enhance Human Performance Based on Phase Oscillators. *J. Mech. Robot.* **7**, 011001.

- Suydam, S. M., Manal, K. and Buchanan, T. S.** (2017). The Advantages of Normalizing Electromyography to Ballistic Rather than Isometric or Isokinetic Tasks. *J. Appl. Biomech.* **33**, 189–196.
- Umberger, B. R.** (2010). Stance and swing phase costs in human walking. *J. R. Soc. Interface* **7**, 1329–1340.
- Umberger, B. R., Gerritsen, K. G. M. and Martin, P. E.** (2003). A model of human muscle energy expenditure. *Comput. Methods Biomech. Biomed. Engin.* **6**, 99–111.
- Welker, C. G., Simpson, C. S. and Hawkes, E. W.** (2017). Simulation of a passive assistive device to reduce running effort. In *Proceedings of the XXVI Congress of the International Society of Biomechanics*, .
- Wells, D. J.** (1993). Muscle performance in hovering hummingbirds. *J. Exp. Biol.* **178**, 39–57.
- Zhang, J., Fiers, P., Witte, K. A., Jackson, R. W., Poggensee, K. L., Atkeson, C. G. and Collins, S. H.** (2017). Human-in-the-loop optimization of exoskeleton assistance during walking. *Science (80-.)*. **356**, 1280–1283.

Figures

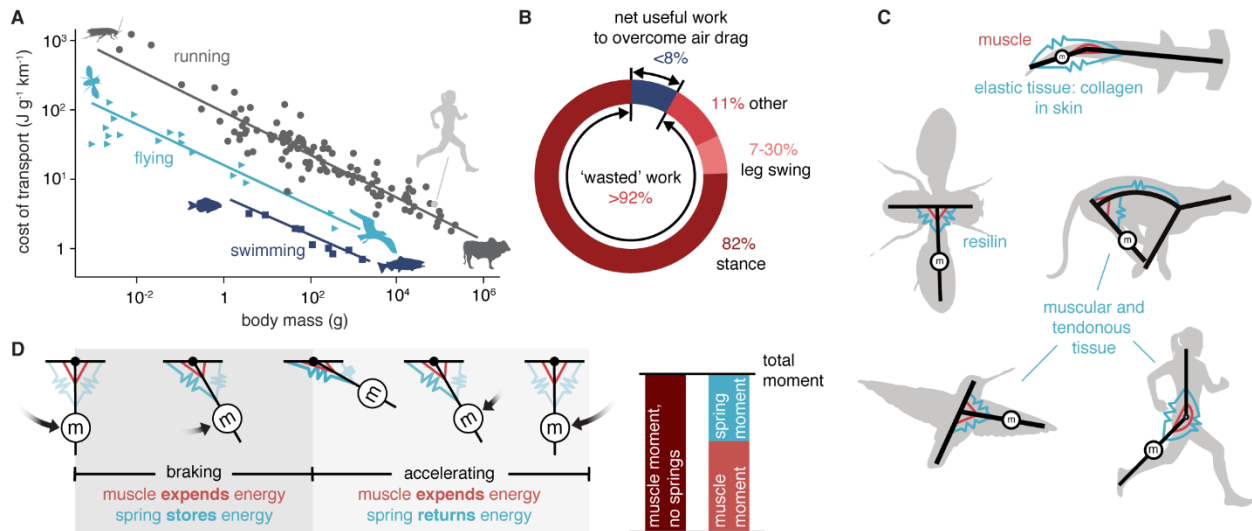


Fig. 1. Energetics and mechanics in running animals. **A**, Cost of transport as a function of body mass (Full, 1989; Minetti et al., 2013; Schmidt-Nielsen, 1972) shows that running (grey circles) is less efficient than swimming (dark blue squares) and flying (light blue triangles). **B**, Only a small fraction of the energy expended in running does useful work on the environment to move against air resistance (Davies, 1980; Pugh, 1970); the remainder is expended primarily to accelerate the center of mass, both vertically and fore-aft, during stance. Much less is used to swing the legs (Arellano and Kram, 2014; Marsh et al., 2004; Modica and Kram, 2005). **C**, Elastic tissues are hypothesized to reduce the energy required to swing limbs. **D**, A pendular model of limb oscillation showing that a parallel spring (elastic tissue) can store energy during braking and return energy during acceleration, reducing required muscle moments.

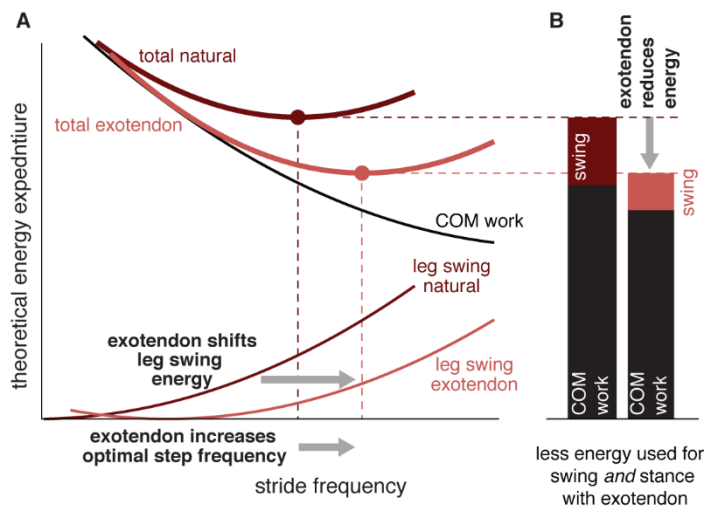


Fig. 2. Exotendon hypothesized mechanism of savings. **A**, Runners choose an energetically optimal stride frequency (dark-red circle), which results from a combination of processes that require more energy with increasing stride frequency, such as leg swing (dark-red thin line), and those that require less energy with increasing stride frequency, such as the work performed to redirect the center of mass during stance (black thin line). We hypothesize that the exotendon shifts the leg swing curve rightward (light-red thin line), increasing the optimal stride frequency, and reduces total energy expenditure (including expenditure associated with work on the center of mass). **B**, Note that at this new optimal stride frequency, the costs associated with performing work on the center of mass can be reduced by an amount that is comparable to, or even exceeds, reductions associated with swinging the legs.

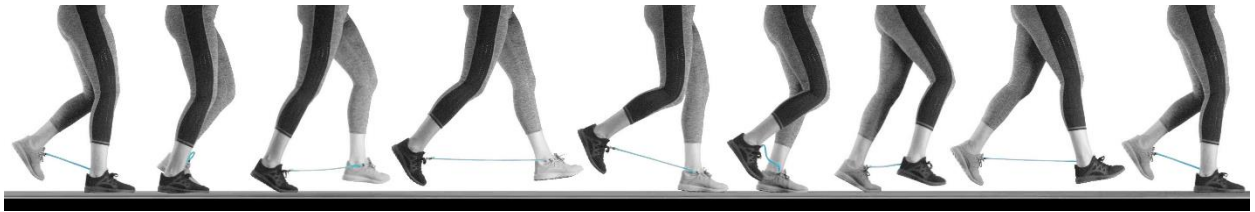


Fig. 3. Time-lapse photographs of a runner using the exotendon. The length of the exotendon is tuned so that the device is long enough that it does not apply forces when the feet cross each other and does not break when the feet are far apart, yet short enough that it does not become entangled when the feet pass each other. Images span one complete gait cycle.

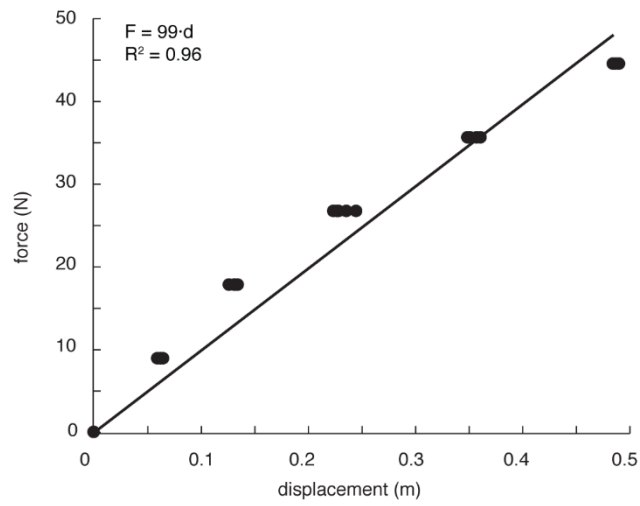


Fig. 4. Exotendon device force-length characterization. The extendon exhibited a near linear relationship between force, F , and displacement, d ($R^2=0.96$).

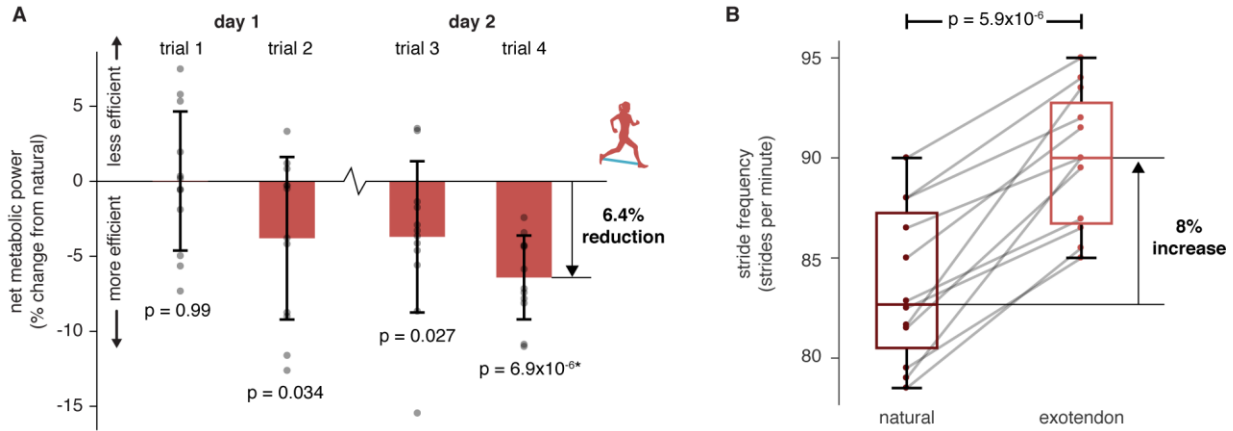


Fig. 5. Reduced energy expenditure during exotendon running (n=12). **A**, On day 1, runners initially showed no change in energy expenditure (trial 1), yet showed reductions after running with the exotendon for 15-20 minutes (trial 2). Runners retained these savings across days (trial 3). After a total of 35-40 minutes of experience with the exotendon across both days, the greatest reductions in energy expenditure were evident (trial 4), with all runners (n=12) showing improved economy and average savings of $6.4 \pm 2.8\%$. Error bars represent one standard deviation. Asterisks indicate statistical significance after Holm-Šidák corrections with confidence level $\alpha=0.05$. **B**, By the final trial participants took shorter, faster strides with the exotendon, increasing stride frequency by an average of 8% above that measured during natural running ($p=1.1 \times 10^{-5}$ two-tailed paired t-test, n=12).

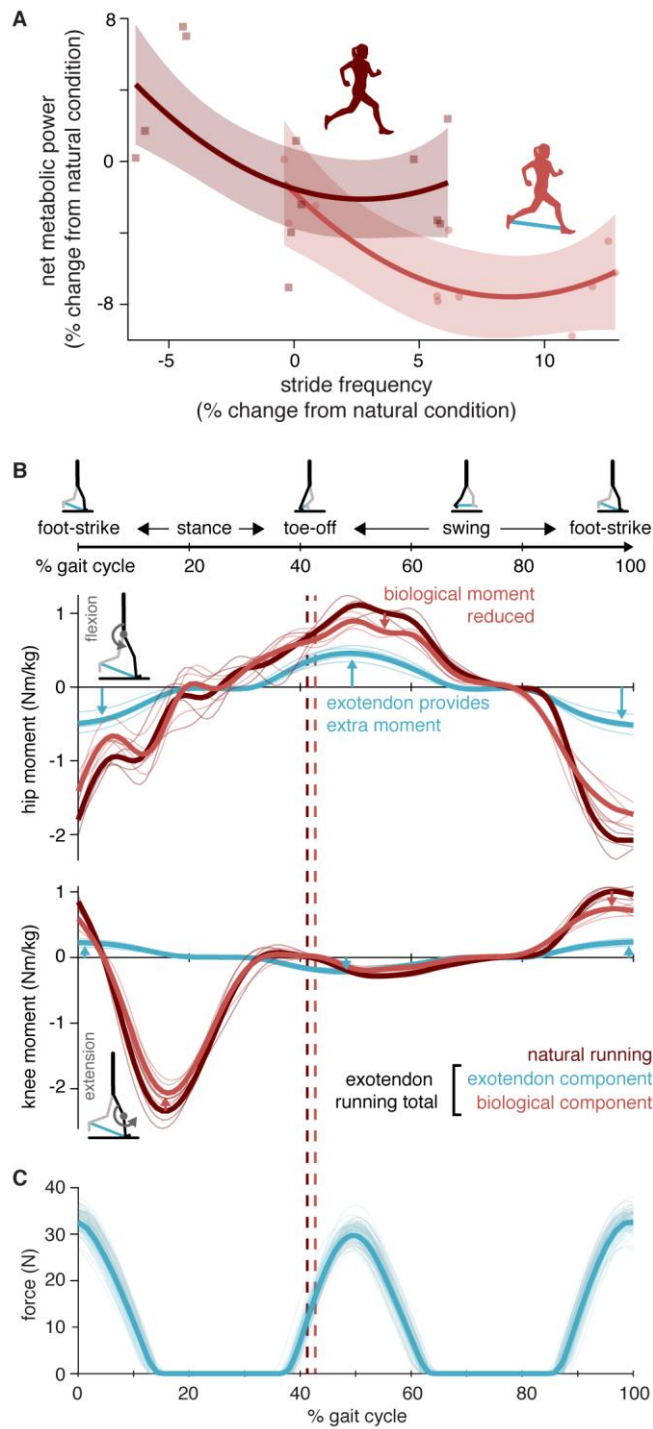


Fig. 6. Exotendon mechanism of savings (n=4). **A**, In experiments, the exotendon increased the energetically optimal stride frequency (8.1%, $p=3.7 \times 10^{-3}$, paired t-test, $n=4$). Faded regions show the 95% confidence interval of curve fits. **B**, Biological moments during swing were reduced,

likely due to the assistance of the exotendon, and biological moments during stance were reduced, possibly due to the increased stride frequency. Note that horizontal forces applied by the exotendon to the stance foot likely do not affect the joint moments of that leg, because they are reacted by frictional forces with the ground. However, the exotendon forces applied to the swing leg may indirectly affect the joint moments of the stance leg through the hips. **C**, Force-time plot of the exotendon throughout the stride for one participant (n=1). The tension in the exotendon peaked at around 30N at the extents of the stride, and was zero whenever the feet were closer together than the slack length of the device.

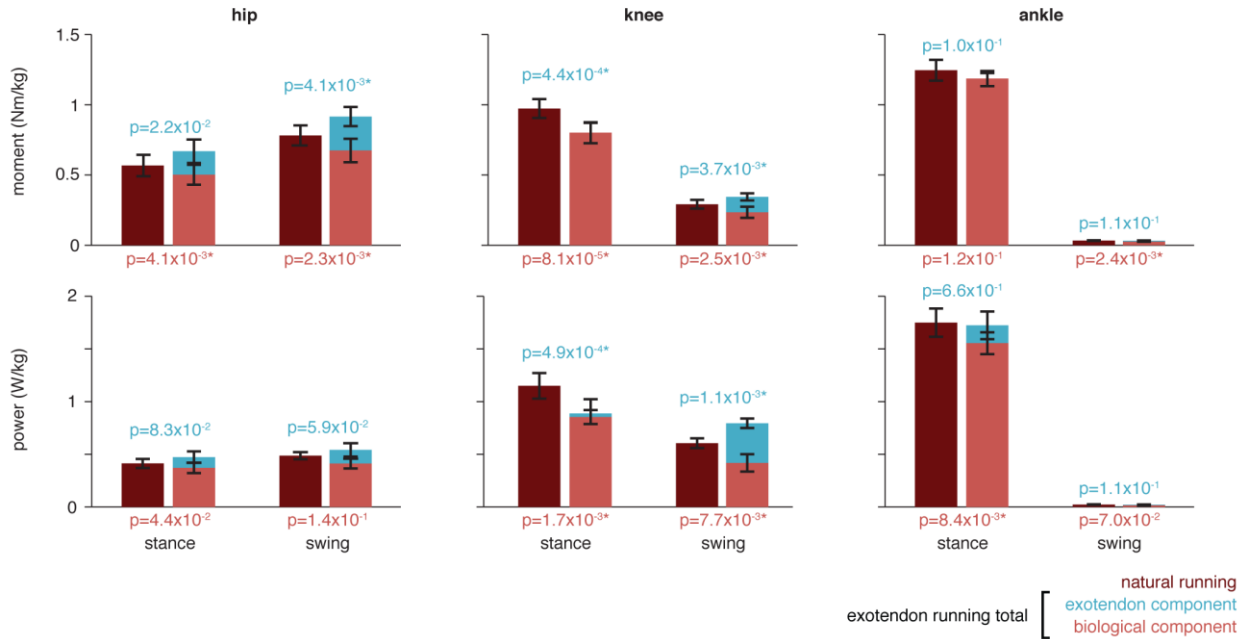


Fig. 7. Average joint-level kinetics (n=4). Comparisons of average, absolute joint moments and powers across stance and swing for the four participants from Experiment 3. We compared moments and powers produced during natural running (dark red) to those produced during exotendon running. Average kinetics during exotendon runs were separated into the exotendon contribution (blue) and the biological contribution (light red). We report the p-values resulting from two-tailed paired t-tests comparing biological contributions to kinetics in natural and exotendon running below the axes (light red text) and comparing total kinetics in natural and exotendon runs above the bars (light blue). Asterisks indicate comparisons that were significant after Holm-Šidák corrections ($\alpha = 0.05$). When running with the exotendon, during swing, hip, knee and ankle biological moments are reduced compared to natural running, as is knee power. During stance, hip and knee biological moments are reduced, along with knee and ankle powers.

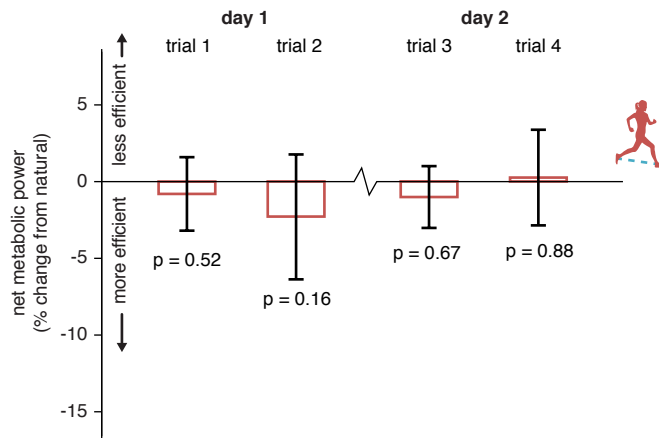


Fig. S1. Placebo test results (n=4). Four participants completed the same protocol as the main experimental group, but were given an exotendon with stiffness less than 5% that of a normal exotendon. These participants showed no change in running economy, relative to natural running, with the placebo exotendon (two-tailed one-sample t-tests). Error bars represent one standard deviation.

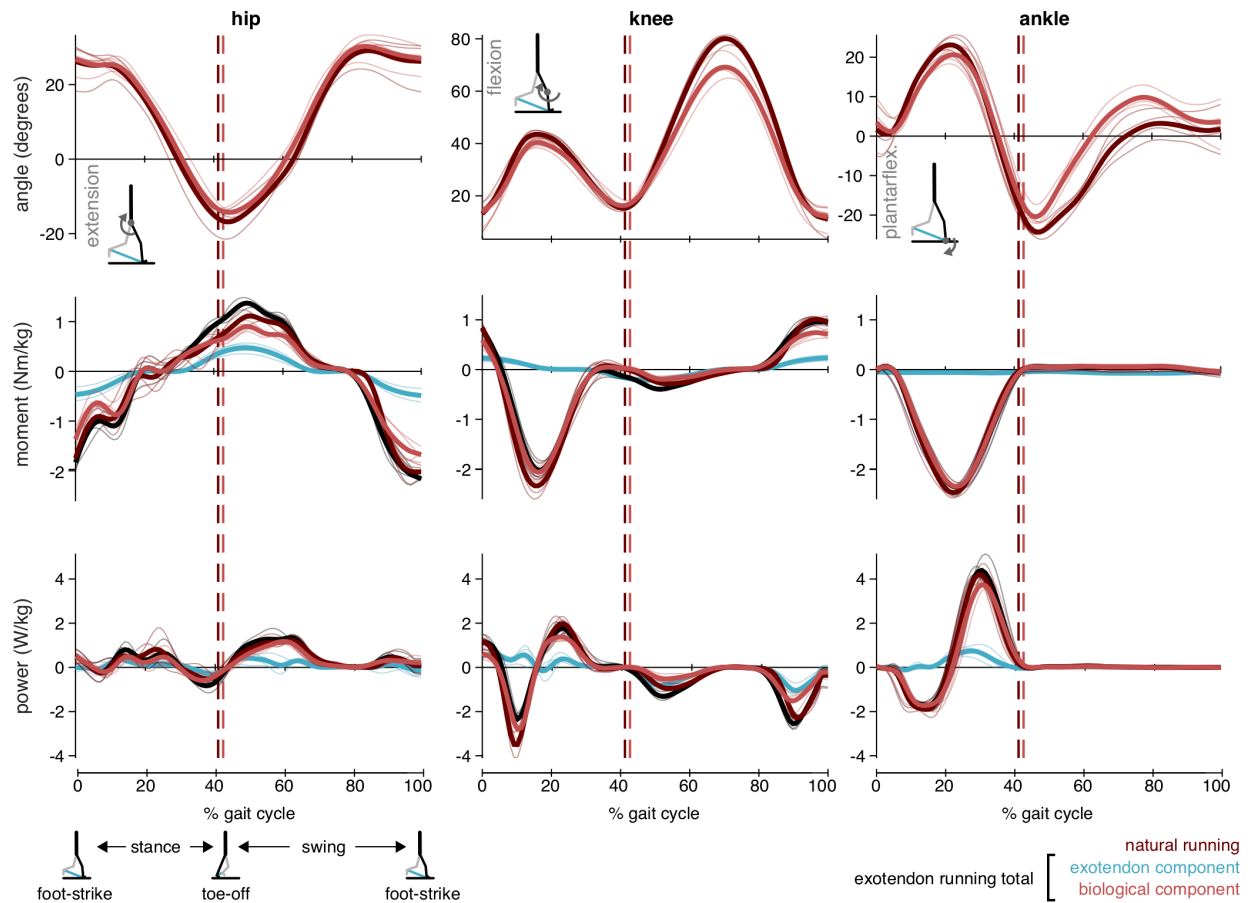


Fig. S2. Joint-level kinematics and kinetics (n=4). Traces show average joint angles, moments, and powers across the gait cycle for natural running (dark red) and exotendon running. Kinetics from exotendon running are separated into exotendon contributions (blue), biological tissue (muscles, tendons, etc.) contributions (light red), and the total joint kinetics (black) for the four participants from Experiment 3. Thin traces show stride-averaged trajectories for individual participants (n=4) while the thick traces show trajectories averaged across participants. Vertical dashed lines indicate across-participant average toe-off time for exotendon running (light red) and natural running (dark red).

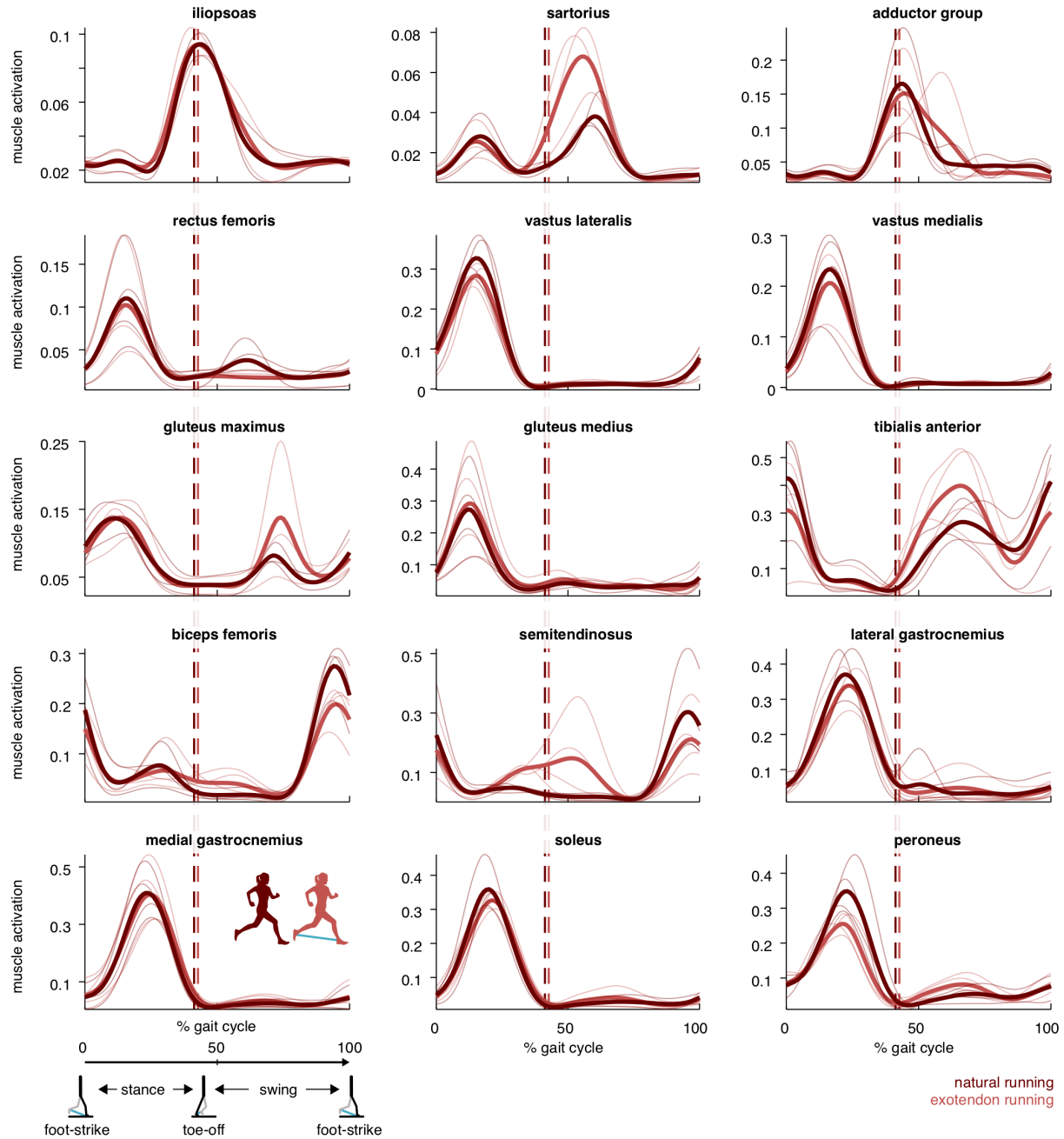


Fig. S3. Muscle activity (n=4). Average muscle activity for each participant (thin traces) and across participants (solid lines) for natural running (dark red) and running with the exotendon (light red) as a function of gait cycle. The vertical dashed lines indicate the average time at which the toe lifts off the ground during exotendon running (light red) and natural running (dark red).

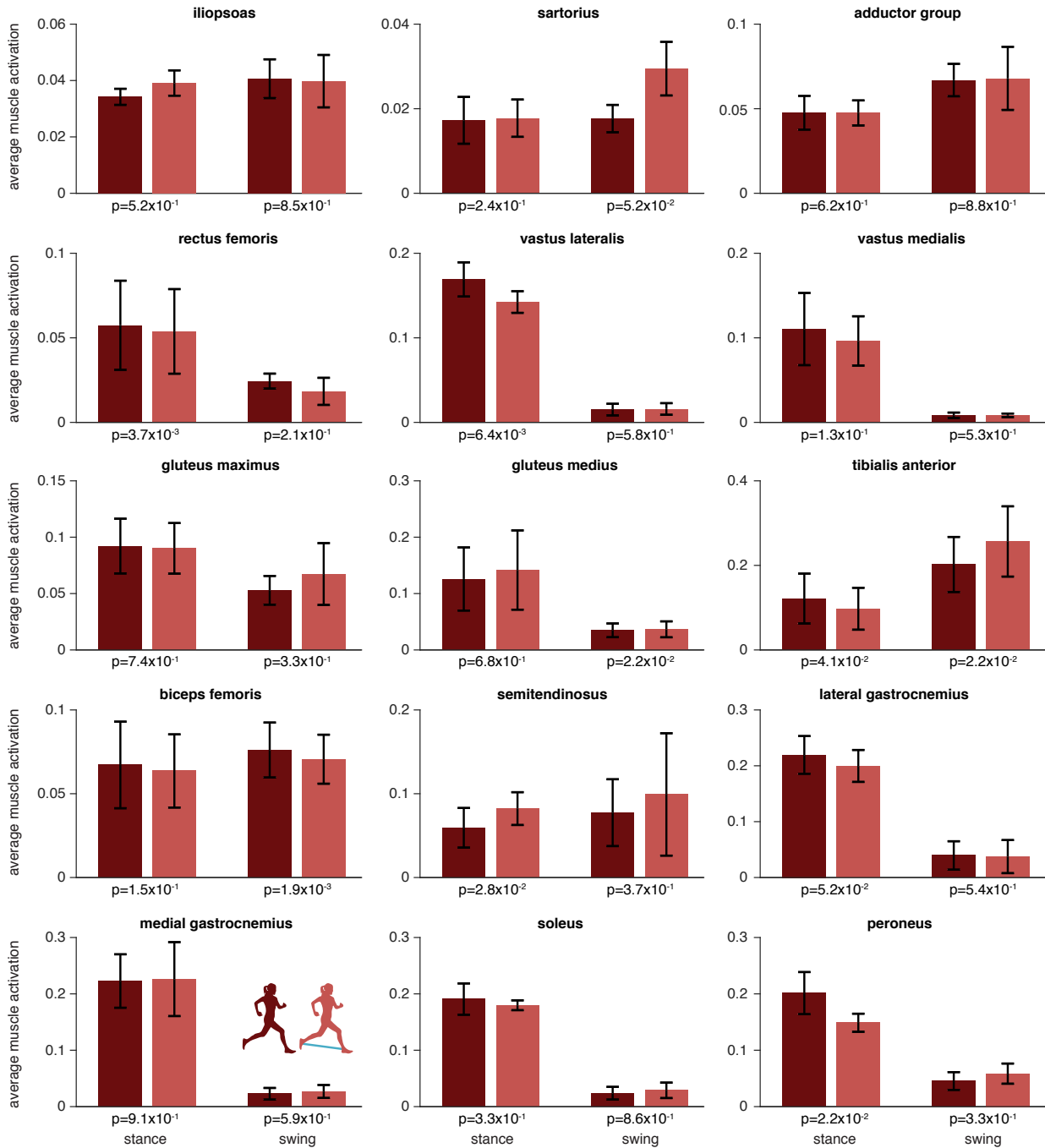


Fig. S4. Average muscle activity (n=4). Comparisons of average, normalized muscle activity, computed from EMG recordings, across stance and swing phases of gait. Statistical comparison (paired t-test with Holm-Šidák corrections, $\alpha = 0.05$) revealed no significant changes in muscle activity as a result of running with the exotendon.

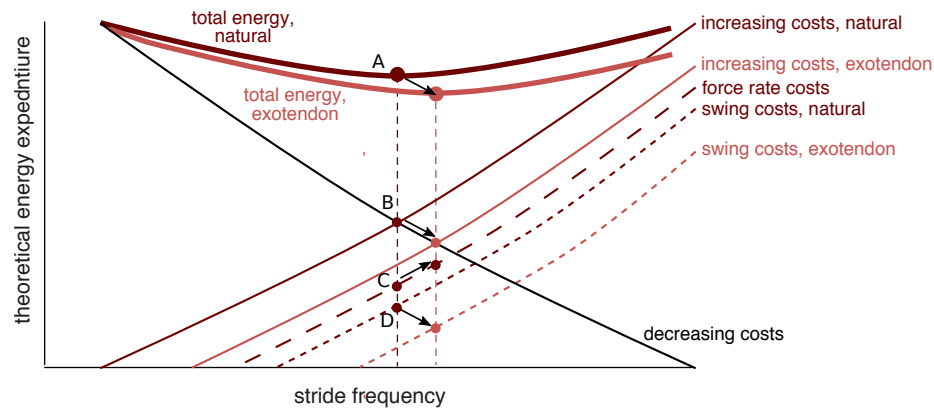
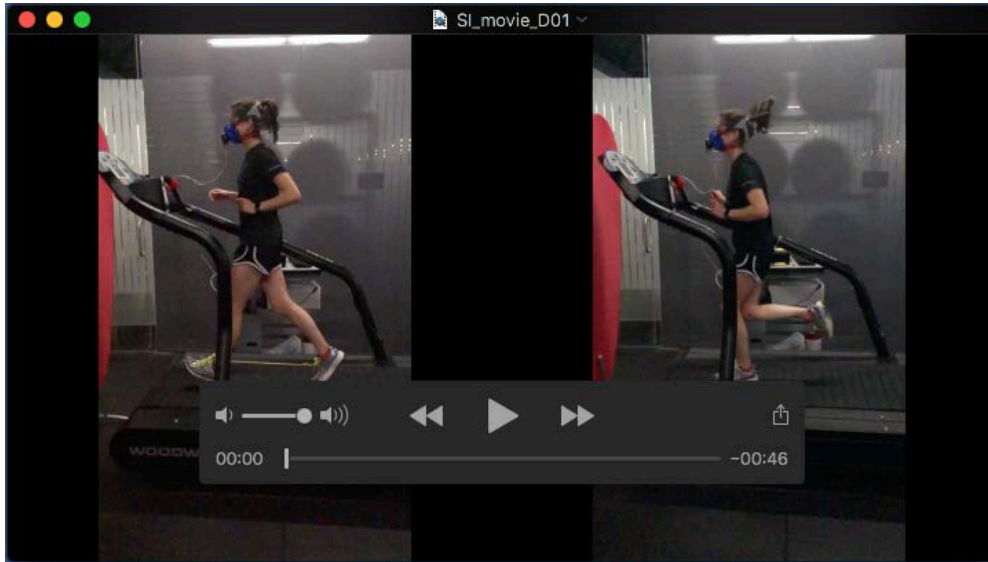


Fig. S5. Exotendon hypothesized mechanism of savings including ‘force rate’ costs. The total energetic cost (bold, dark red line) comprises costs that increase with stride frequency (thin, dark red line), and costs that decrease with stride frequency (thin, black line). The *increasing costs* can be broken into subcomponents, here *force rate costs* (long dashed, dark red line) and *swing costs* (short dashed, dark red line), although others could be added as well. When the exotendon assists leg swing, the *swing costs* subcomponent line shifts (short dashed, light red line). This in turn shifts the net *increasing costs* line (thin, light red line), resulting in a new total energy curve (bold, light red line), and a new the optimal stride frequency (vertical, dashed light red line). The operating points on the curves of both the *increasing costs* and *decreasing costs* (Point B) as well as on the total energy expenditure curve (Point A) shift down and to the right with the exotendon, as does Point D (the operating point on the curve of the *swing costs* subcomponent of the *increasing costs*). The net savings in energy expenditure occurs despite Point C (operating point on the curve of the *force rate costs*) shifting up and to the right. Thus, even though some costs might increase with adaptation to the exotendon, decreases in other costs can result in net savings.



Movie 1. Running with the extotendon.